Single Mode Autonomous Solar Spectrometry

Tamara Nelson, Kara Semmen, Misael Salazar, Jarolin Jimenez Vasquez, and Miguel Daboin

Dept. of Electrical Engineering and Computer Science, University of Central Florida, Orlando, Florida, 32816-2450

***Abstract* — This paper covers the design process and fabrication of a research system with a focus on monitoring and observing the sun's spectrum. This consists of two significant factors: a single-mode spectrometer and a Fabry-Perot etalon for calibration, both and autonomous rooftop housing to consistently track the sun and provide protection of a mini telescope previously designed by CREOL's Astrophotonics research group. The raw data from our system and the designs achieved will be collected and expanded upon by the research group for further study of the sun's characteristics.**

I. Introduction

The current state of space exploration has researchers searching for other solar systems and planets with similar characteristics to the Earth. One such attribute is that it must be an exoplanet, orbiting a star. Beneficial research for such discoveries includes the study of the characteristics of the sun to have a comparison for other stars in the galaxy. Due to the solar system's gravitational pull, the barycenter constantly changes position, from the center of the sun to outside of it. This causes extra movement of the sun, so that it is not only rotating, but also wobbling around the barycenter. One method of studying the sun is its redshift. [1,2] This can be accomplished through observing the sun's spectrum.

Our project was requested and sponsored by Dr. Stephan Eikenberry of the Astrophotonics research group in CREOL to design a system that consistently monitors the sun to collect raw data of the sun's spectrum and capture images of the sun's surface. To accomplish this, we were requested to design two key portions of the project, as demonstrated in the figure above: a rooftop system meant to hold the solar imager and the telescope (already designed by the research group) and the laboratory system that filters the light.

The rooftop system has automatic tracking that accounts for the movement of the sun, and a solar imager is meant to capture the sun's unpredictable surface activity to compare with the spectrum at that moment. The rooftop system was also designed to remain weather protected to ensure its longevity. A single mode spectrometer, paired with a Fabry-Perot etalon (for calibration), was requested to collect light from the rooftop system to observe the sun's spectrum. [3]

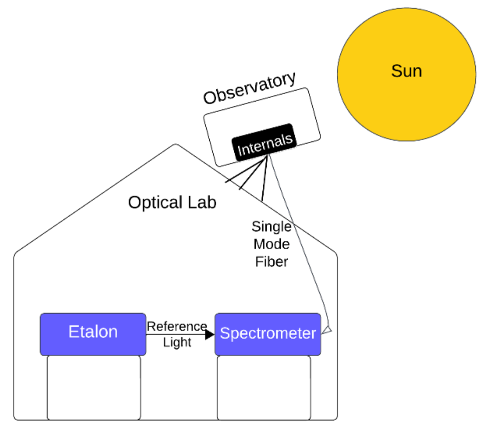

Fig. 1 Connection between the rooftop system and the laboratory system, highlighting the requested structure of the project.

II. Laboratory system

A. Spectrometer

The optics of the cross dispersed echelle spectrograph includes the following primary components: Two canon lenses, a reflective echelle grating, a 50 mm glass prism, and two single mode fibers (one with light from the rooftop telescope and one from the Fabry Perot Etelon). These are mounted onto an aluminum plate with mounts designed for this system.

The spectrograph being used for this project is called a cross dispersed echelle spectrograph. This system utilizes two diffracting optics: a prism and a reflective echelle grating. The echelle grating has a very course groove density, with the grooves engraved at an angle. This grating provides high resolution with small bandwidth. The zeroth order of the diffracted light is then incident onto a prism, which disperses in a different direction to the initial echelle grating. This results in a two-dimensional spectrum with a very small bandwidth in one direction and a much broader bandwidth in the other. This preserves a higher resolution while obtaining the bandwidth needed. The initial calculations for this spectrometer are based off the desired magnification, resolving power, bandwidth of the system, and peak wavelength which are 3.5x, 50,000 (minimum), 400-700 nm, and 532 nm, respectively. These values are used to calculate: 1) the pitch of the echelle grating 2) the necessary focal lengths and F/#'s of the collimating and camera optics, 3) the type of fiber used to feed light into the system, and 4) the sensor used. These values are determined primarily from the below equations:

$$R = \frac{\lambda}{\Delta\lambda}, \tag{1}$$

$$m\lambda = \sigma(sin\alpha + sin\beta), \tag{2}$$

$$M = \frac{f'}{f} \text{ and,} \tag{3}$$

$$NA = \frac{D_E}{2f}. \tag{4}$$

Where R is resolving power, lambda is the peak wavelength of the light, delta lambda is the bandwidth, m is the diffraction order, σ is the groove density of a grating, α and β are the incident and reflection angles of the light on the grating, M is magnification, f' and f are the back and front focal lengths of the optical system, NA is the numerical aperture of an optical component, and D is the diameter of the entrance pupil.

While performing these calculations it is important to not only ensure that the given specifications are fulfilled, but also to choose and place components in correct relation to one another to optimize light throughput and minimize aberrations. When choosing the optical fiber and collimating lens, the numerical aperture of the optical fiber should have the same numerical aperture as the collimating lens so that no light is lost. The resulting optics chosen were an SM400 single mode fiber with a numerical aperture of 0.13, a reflective echelle grating with a groove density of 31.6 grooves/mm and a pitch angle of 63.5 degrees, a collimating optic with a focal length of 87 mm, a 50 mm F2 prism, a focusing lens with a focal length of 305 mm, and an atik CMOS sensor with pixels 3.5 microns wide, and a sensor which measures to be about 35 mm wide. The echelle grating must be tipped back at an angle of 63.5 degrees to the incident light, as this is the angle that the grooves are etched. A single mode fiber is used for this system rather than a multimode fiber to maximize the resolution of the system.

This system is then put into ZEMAX, an optical ray tracing software. The system initially is entered in paraxial mode. This is to ensure that the desired specs are indeed fulfilled with the calculated values in a perfect system. To ensure that the zeroth order from the echelle grating is directed in the prism, the calculations are performed for the "Littrow Configuration", where the reflected angle is equal to the incident angle. This means that the diffraction order that is being observed is reflected into the light source. The echelle grating is tilted until this diffracted light is steered away from the light source, just far enough so that the proceeding optics can be placed in the beam path without getting in the way of the fiber and collimating lens. This creates the "Quasi-Littrow Configuration." Note that the echelle is tilted for beam steering on a different axis than when it is "tipped" to match its groove angles. To avoid confusion, we use the term "tip" to refer to the 63.5-degree groove angle, and "tilt" to reference the beam steering angle. Finding the best value for tilting the echelle grating is observed in the Zemax software, as the angle of reflected light from the echelle grating can be tested and directly observed quite easily. Upon testing various angles and configurations and considering the size of the prism and camera optics and mounts, the grating was decided to be tilted at 13 degrees to the incident beam.

The next step involves expanding the Zemax design to include real optics and optimizing the collimator and camera optical designs. The system must be optimized for all wavelengths in the desired bandwidth, and resolution. A system of lenses was designed for the collimator and camera portions of the system. However, this design requires many custom ordered lenses, which greatly drives up the cost and timeline for completing the final product. An alternative, cost effective method was to utilize Cannon camera lenses. These lenses are low in price and fulfill the requirements for the camera and collimator portion of this project. The full optical design will eventually be implemented by the CREOL Astrophotonics laboratory as their research progresses.

To ensure proper alignment, a mounting plate and mounts were designed by importing a solid ray model from the Zemax ray trace of the system into SolidWorks. The placement and height of mounts were based around the Zemax ray trace. Once all mounts were placed and mated, the hole wizard function in SolidWorks was used to place holes in the modeled mounting plate in the correct locations. The mounts for the grating and prism were 3D printed, while the load-bearing mounts (holding the Canon lenses), and the base plate were machined out of aluminum. The ray trace glitches slightly when it reaches the prism, but the ray path and design are not affected.

Figure 1. SolidWorks model of Spectrograph System.

The single mode fibers are connectorized together and mounted in front of the collimator lens as the light source of this system. On the other end of the fibers, one is spliced to the solar telescope, while the other is mounted and receiving output from the Fabry Perot Etalon system. The Atik camera sends the resulting data to its corresponding software, Artemis Capture. This is where the data will be recorded and observed by the CREOL Astrophotonics research group.

B. Fabry-Perot Etalon

The main purpose for the Fabry-Perot etalon is to act as a reference input of the spectrometer to determine how much the sun's spectrum shifts. The Fabry Perot Etalon design is an optical cavity, or resonator, characterized by free spectral range, linewidth, and finesse.

The first stage of the design was to determine the necessary criteria for spectrograph calibration. Based on our research into pre-existing calibration methods and the guidance of our sponsor, the etalon's free spectral range should be 3-5 times the resolving element of the spectrograph, this will be referred to as the multiplier. Knowing the spectrograph's resolving power, we were able to calculate the corresponding free spectral range of the etalon using the equations below.

$$R = \frac{\lambda}{\Delta\lambda_{res}} = \frac{v}{\Delta v_{res}} \tag{5}$$

$$\Delta v_{res} = \frac{v}{R} \tag{6}$$

$$FSR = \Delta v_{etalon} \approx m \cdot \Delta v_{res}. \tag{7}$$

Where m is the multiplier, $\Delta\lambda_{res}$ is the resolution element in wavelength, Δv_{res} is the resolution element in frequency, and Δv_{etalon} is the FSR in frequency. We consider the etalon in the frequency domain for this design. We use a central wavelength of approximately 500 nm, where v becomes 6×10^{14}. With a resolving power of 10^5, the resolution element is equal to 6 GHz. Since we have a range of options for the FSR, we calculated it with both 3 and 5 as the multiplier, with results of 18 GHz and 30 GHz, respectively. From here we calculated the required linewidth specification. To prevent line blending, we needed a linewidth that is significantly narrower than the etalon's FSR and the spectrograph's resolution element. So, we aimed for a maximum FWHM of $\Delta v_{res}/10$, with a goal of less than $\Delta v_{res}/2$. The last determining characteristic for the etalon is the finesse. Increasing the finesse decreases the loss that occurs in the cavity, so to maximize the output power, we aim for a higher finesse. Utilizing the criteria, we were able to select a range of reflectance of 86%-95%.

Within the selected reflectance range and wavelength range of 400 – 700 nm, there is a limited selection of mirrors. The chosen mirror was determined by these factors. We calculated that the chosen component would be compatible using the equations for FSR, FWHM, and in MATLAB. With mirrors of a 98% reflectance, we achieved an FSR that matches the criteria, a FWHM that is less than the goal, and a higher finesse than expected. Using two of these mirrors 5-8 mm apart would be compatible with the spectrograph. Below is a table of the ideal criteria and the actual calculations given the chosen mirrors to match such criteria.

	FSR (GHz)	FWHM (GHz)	F	R	Cavity Length (mm)	Range (nm)
Goals	18 - 30	< 0.6 - 3	>25-50	86%-95%	5 - 8 mm	400 - 700
Actual	18.75 - 30	0.12 - 0.19	160	98%-99%	5 - 8 mm	400 – 750

Fig. 2. Comparison of ideal and actual calculations, where F is finesse and R is the mirror reflectance.

When constructing the etalon, we started with mounting the mirrors in kinematic mounts and aligning them with a HeNE laser. This was to ensure that the mirrors are parallel. The output beam was observed to flicker as the cavity length was adjusted. With the mirrors parallel, we were able to switch out the light source for a 4900K white LED with an output power of 740 mW. A high output power was chosen to accommodate for the high loss in an etalon of 160 finesse. The white LED paired with an aspheric collimation lens with an antireflective coating over 350 – 700 nm. The collimated beam is positioned to enter the etalon. The output from the laser alignment and the white light source are shown below. When the cavity is positioned at 6 mm, the etalon will meet its criteria.

Fig. 3. Output of the etalon with (left) a 633 nm laser input and (right) the collimated LED input, utilizing a focusing lens for detection.

The next challenge was to couple the output of the etalon into the single mode fiber. The focal length of the lens used must correspond to the mode field diameter of the fiber. With knowledge of the diameter of the input beam (20 mm) and the mode field diameter (3 µm) we were able to calculate a focal length of approximately 300 mm. However, we have realized that this distance is too far to effectively focus the diverging output. Another option is to include an aperture stop to control the diameter of the input beam of the last focusing lens. This would have minimized the focal length needed to couple the output into the single mode fiber that feeds into the spectrometer. The design for the etalon is shown below.

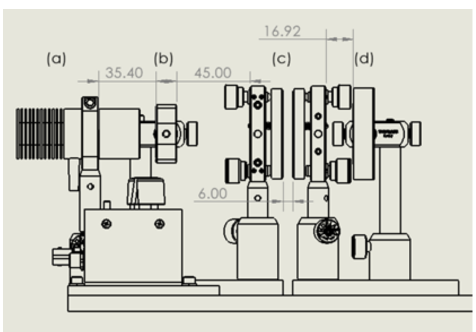

Fig 4. Design of the Fabry-Perot Etalon with distances (mm): (a) LED, (b) collimating lens, (c) parallel mirrors, and (d) 50 mm diameter focusing lens

The Fabry Perot Etalon is highly sensitive to environmental factors, such as temperature and acoustic vibration, that effects the stability and precision of the resulting design. Considering that the stability of the etalon was the greatest challenge, we also have many other alternatives and/or plans for how it can be improved. This includes a plexiglass box set over the whole laboratory system, with a coating of foam to account for acoustic vibration. Additionally, Mylar can be layered over the outside to aid in temperature controlling both optical systems. An additional design, though unimplemented is the incorporation of hollow fiberglass triangles on each side of the etalon to absorb acoustic vibration. [4]

These designs have been heavily considered, but due to a lack of time and realistic resources, we settled on a basic anti-thermal mounting design. The final design is built on machined plates of aluminum. The plates are stacked and mounted to counteract linear thermal expansion, as shown in the design below. This aids in increasing the stability of the cavity lengths when undergoing temperature fluctuations.

III. HARDWARE

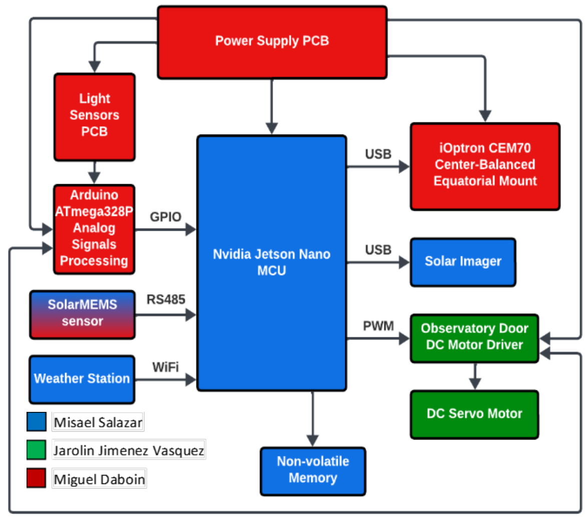

Fig 5. Hardware Components Block Diagram

A. *Hardware Components*

For our project, the selection of a microcontroller was an important decision that influenced the overall design and functionality of the system. We chose to use the NVIDIA Jetson Nano, which was highly recommended by our mentor, it is a powerful and compact computer capable of executing multiple tasks simultaneously. The Jetson Nano was integrated with many components to form a fully autonomous observatory.

The NVIDIA Jetson Nano was a clear choice due to its superior overall capabilities. It offers a powerful processor, low power consumption, and plenty of I/O devices for us to use. We used the processing power to achieve our goals of capturing high resolution solar images, analyzing, and predicting the weather, and controlling the mechanical parts of our observatory. The Jetson Nano also has the ability to extend its nonvolatile memory by using an SD card. We chose to use a 256 GB SD card to provide plenty of storage space for all of the data we plan on collecting from our sensors.

The solar imager we chose was the Celestron NexImage 5. The NexImage 5 is a 5 Megapixel (MP) camera that contains a special kind of CMOS sensor that reduces noise levels in the image. It also has the exact pixel size we needed of 2.2 microns squared. The solar imager connects to the Jetson Nano by USB, enabling us to take high resolution images of the sun.

We used a dedicated solar sensor in combination with our own light sensing PCB to maintain a proper alignment with the Sun's precession. The sun sensor we used was the Solar MEMS Sun Sensor ISS-DX. This sensor communicates to our Jetson Nano by using the RS485 communication protocol, telling us the current light intensity, which we expect to give use peaks when properly aligned with the sun. We used our own specially designed light sensor to determine which direction our system should move. The data from the sensor we designed told us the specific direction to drive the mount, and the sun sensor we purchased would tell us when we were properly aligned.

To ensure that the observatory would be protected from a range of different weather conditions, we incorporated a weather station into our design. In this case, we chose to use the WS-2000 AmbientWeather Weather Station. This weather station communicates with our Jetson Nano via Wi-Fi. Our Jetson Nano acts as a server that then receives the data from the weather station. The Jetson Nano then uses the data from our weather station to predict the weather.

The NVIDIA Jetson Nano's integration into our system serves as the central hub for communication and control. Its robust processing power and versatile connectivity options enabled seamless interaction between the hardware components, thus fulfilling the project's requirement for a reliable and efficient automated observatory system.

One of the most critical parts of the solar tracker system is the mount and the dual-axis movement. For our previous design, we had decided to create a dual-axis platform with two stepper motors in charge of the movement of each axis and to point all the solar spectrometry roof components out to the sun. As a request from out Sponsor, this component design was replaced with the iOptrom CEM70 equatorial mount that provides a more accurate and precise movement of the platform. The iOptrom CEM70 is equipped with precision stepper motor with 0.07 angle degrees accuracy for precise and accurate tracking. The mount is connected to the Nvidia Jetson Nano which controls its movement based on the data received from the Light Sensor PCB and the SolarMEMS device.

B. PCB Designs

Due to the required level of electrical design, we used Altium Designer Professional software to create both the Power Supply and the Light Sensor PCB designs. This software allowed us to get access to real-time libraries for the all the components we needed and made the whole design process much easier and smoother.

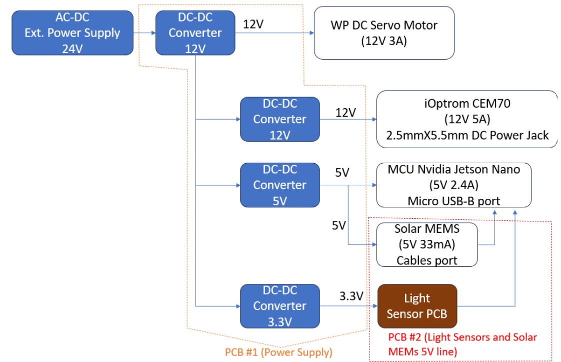

Fig 6. PCBs Block Diagram.

For our main power supply system, we designed a PCB with the capability to provide several required voltage outputs to the solar tracker system and MCU components. It provides 12V 5A to the iOptrom CEM70 equatorial mount through a DC power jack connector; 12V 3A to the DC motor responsible of opening/closing the door of the roof system box and protecting the main components; 5V 2.4A to the Nvidia Jetson Nano MCU through micro-USB; 5V 33mA to the SolarMEMS device and 3.3V 2A to the Light Sensor PCB which also acts as a bridge for the RS-485 connection.

The Power Supply PCB v3, which we will be referring to as PCB#1, makes use of four voltage regulators IC: two XL4015E1 and two XL4016E1 which are high efficiency components and allow us to adjust the voltage ranges as we had to take care of voltage drop issues from Power Supply PCB v2.2.

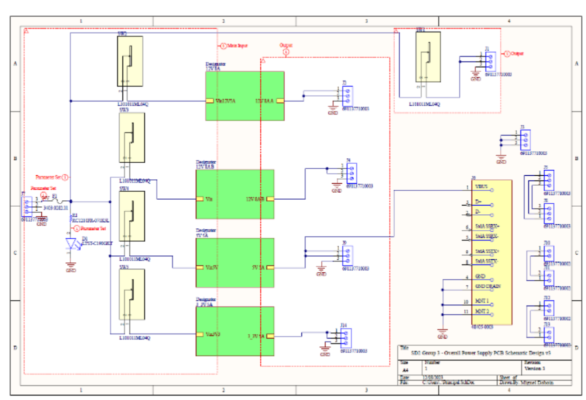

Fig 7. Power Supply PCB v3 Overall Schematic.

One example is the Nvidia Jetson Nano that, after being connected to the voltage supply line, caused a voltage drop from 5V to 4.74V on the Power Supply PCB v2.2. For this, we designed a version 3 of the Power Supply PCB by replacing the voltage regulators IC from LM2678T to XL4015E1 and XL4016E1. This way and with the new designed, we managed to solve all the issues from previous designs and perfected the layout of components getting by result a pretty reliable and an efficient Power Supply PCB design.

The above Fig. 7 shows the overall schematic for our Power Supply PCB v3 made using Altium Designer Professional software. Consider that the green boxes are the designators for each one of the voltage line suppliers (which means that, inside of each box, it is different voltage line schematic). This PCB is supplied by an external 120VAC/24VDC power supply with IP67 certification needed for our project requirement to be weather/water resistant. On this design, we also added decoupling capacitors to stabilize voltage supply, fuses to protect the PCB#1 from the 24VDC external voltage input and to also protect the components we are providing power, green-LEDs and switches to acknowledge and control whether a voltage line is on and working well. See below Fig. 8 for a 3D view of the Power Supply PCB.

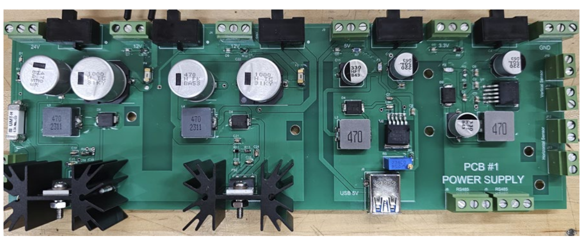

Fig 8. Power Supply PCB v3 Physical view.

Considering the need of having a first device to be able to align all the components on a first-stage positioning before using the SolarMEMS device, we designed the Light Sensor PCB (PCB#2).

This PCB is an analog light tracker which sends voltage high/low signals to the MCU. It was designed as a window comparator circuit. In order to sensing the light, we used simple photocells or photoresistors which is a completely passive device and has no polarity. It has two-axis (vertical and horizontal) with two photoresistors each and the way it works is that if one of them receives more light than the other (same-axis), it will suddenly change the voltage and, by using a comparator, we can easily decide in which direction we need to move the platform, so all the sensors balance the light voltage values again.

For a quick explanation on how the Light Sensor PCB works, we can say that each axis is a circuit employing a comparator, a sensor voltage, and two fixed voltages (window comparator definition). The fixed voltages establish the upper and lower boundaries for the acceptable signal voltage range. Should the signal wander beyond these boundaries, the comparator output undergoes a change, effectively serving as an alarm for the system and sent to the MCU. This lets us to independently assess each comparator to determine whether the sensor signal has deviated excessively in the higher or lower direction. See below Fig. 9 with the Light Sensor PCB v2 design 3D view.

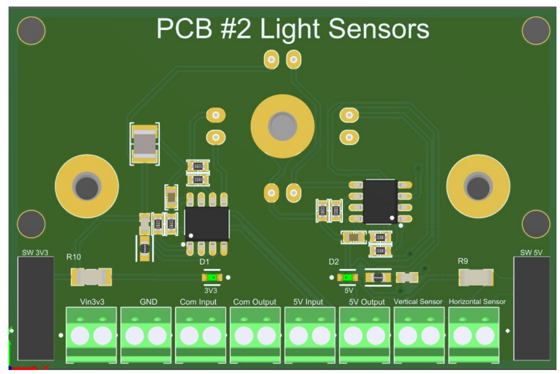

Fig 9. Light Sensor PCB v2. 3D view.

The PCB#2 is placed on front of the plexiglass box together with the SolarMEMS device so they can have the full visibility of solar light and could work properly. Also, this PCB#2 is powered with the 3.3V voltage line from the Power Supply PCB v3. On top of that, the SolarMEMS RS485 data transmission is connected to PCB#2 through extra terminal ports and the signals are send to Power Supply PCB#1 v3 and therefore the Nvidia Jetson Nano.

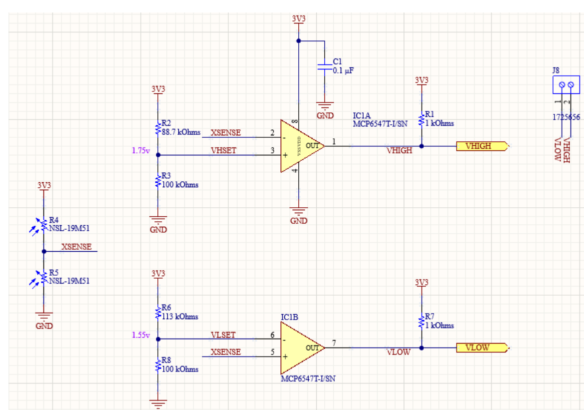

Fig 10. Light Sensor PCB#2 v2 Schematic: Window comparators.

The above Fig. 10 shows the overall schematic for our Light Sensor PCB#2 made using Altium Designer Professional software.

One of the issues we had with this PCB#2 was that the photoresistors were not able to detect the correct alignment because all the photoresistors were receiving the same light intensity from the sun. From here, we designed an object on SolidWorks software that allows us to make axis photoresistors independent from each other and to differentiate on which direction the iOptrom must move. This object is 3D printed and placed on the back of the PCB#2 (where photoresistors are located). See below Fig. 11 with a 3D printed view of the object placed on the back of PCB#2.

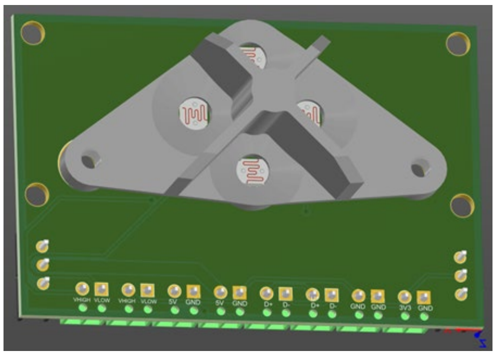

Fig 11. 3D printed object on top of photoresistors. Light Sensor PCB#2 3D view.

Please, refer to the Hardware Block Diagram in Fig. 5 to get a better understanding on how all the electrical components and solar tracker hardware is integrated.

C. Roof system structure

For the system structure we decided that based on what we need it to accomplished of always having the micro telescope looking at the sun as well as having the system be weather protected, we used plexiglass as the material for our box structure, mainly because it is see through, it was easy to work with, to create the box we need it to have our components in, and a good material for the structure we need it. our box consisted of a 24"X16"X12". Each of the plate used for the structure of the box are ½ an inch thick, bolt in together. Below Fig. 11 (Solid Works) is an image of the solid works sketch that we used to create our structure and have the exact measurements need it.

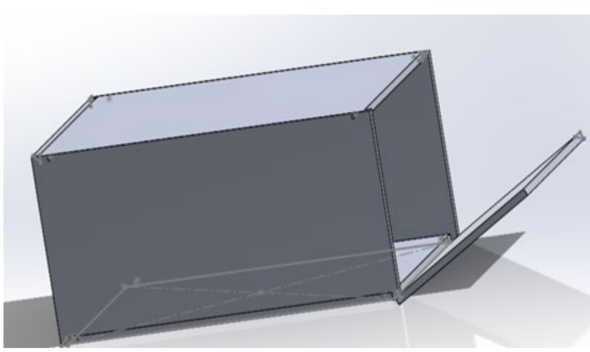

Fig 11. Box designed in Solid Works

Our box is attached to the iOptron mount that is controlling the movement of it so that it can always be pointing towards the sun. We used a slide into a rod mechanism attached to a metal plate which was provided by the grad students that will be using this system for future research after we hand it over to them.

As mentioned before our system is weather protected and besides having the weather machine connected to the system, we planned to have a motor and motor driver operating on the door of the box. Whenever the weather station detects any extreme fluctuation in the weather and, based on the specifications added to the program, the mechanism of the box front door closes, protecting our components from any hazardous weather conditions. Knowing how unpredictable Florida weather is and how this system will be on top of the CREOL building. The motor we first looked and used in our system for this portion of the system was the ECO-Worthy Linear Actuator DC Motor. It has a temperature tolerance range between -65F to 400F degrees which makes it a perfect addition to our project and weather resistance requirements. After having several complications with the integration of the previous motor selected during research (DC Servo Motor) and its controller, we changed our direction as far as what to use for the door mechanism of our structure and end it up using this linear actuator instead, which was easier to manipulate as well as able to easily select a controller board that we could integrate with an Arduino Uno board. We went with this choice for accuracy and precision due to the importance of our system's protection from hazardous weather. The design of the box was with the main intention of weather protection since this part of our system will be on the roof at all times, as well as resistivity, plus clear visibility of the sun.

Besides having the door of the system closed due to the weather, it was programmed to close when the sun was down for the day. So, the door of the system will be open from sunrise to sundown. This way the power consumption of the system can be better controlled, and we were able to stay within the range of power consumption of less than 100 Watts for the power supply side of the PCB.

IV. SOFTWARE

The software component of our observatory was integral to achieving our project's goals. We needed to write programs to read the data from each of our sensors and to control the peripherals we used. We needed to write programs to read the data from each of our sensors and to control the peripherals we used. The NVIDIA Jetson Nano comes bundled with the NVIDIA Jetpack SDK, a full development environment for building applications on the Jetson Nano. The JetPack SDK includes a Linux kernel, with an Ubuntu desktop environment as recommended by our project's sponsor, Dr. Eikenberry.

The software was designed to have a modular approach, allowing each script to operate independently. This ensures that each function of our observatory is independent of the others, and we can individually test or tune them. This modular approach not only made maintenance and upgrades easier, but also allowed the for parallel development and testing of different system components. Each module could be developed, tested, and optimized in isolation before being integrated into the broader system, thus minimizing interdependencies that could cause errors or performance bottlenecks.

To read data from the Solar MEMS Sun Sensor, we wrote a program in Python that would read and write data through the computer's serial ports. We start the sensor by writing a string of hexadecimal values that are defined within the sensor's user manual, then continuously read the data from the port at specific time intervals. To get the data from the weather station, we had to open a port on the computer, that would allow the weather station to connect to the Jetson Nano. Then, the program simply opened a socket on that port, that would allow us to read the weather data. Finally, for our own light sensor, we simply read the values at the given GPIO pins to determine the directionality of the light source.

For the weather prediction, we wrote a simple linear regression model. This model was trained on historical weather data and used on real-time data from our weather station, predicting weather patterns with a focus on variables most relevant to our observatory's operational needs. The model's predictions were used to automate the decision-making process for opening and closing the observatory door, as well as adjusting the solar imager's settings to account for expected changes in sunlight and weather conditions.

Our software's modularity, combined with the powerful features of the Jetpack SDK and the versatility of Python, created a robust and adaptable system. It was capable of not only fulfilling its current requirements but also accommodating future upgrades and enhancements to the observatory.

CONCLUSION

The SMASS system has multiple intricate parts designed to gather data from the sun throughout the year. This is a high resolution, high bandwidth spectrometer device which utilizes single mode fibers rather than multimode fibers to increase the resolution capabilities of this system. In addition, it is designed to track the sun movement through two solar light detection systems and, the components allocated on the roof, are weather protected within a plexiglass box. The results from this project will be handed off to the Astrophotonics research group, who will continue to expand on this project.

THE ENGINEERS

Jarolin Jimenez Vasquez is planning to graduate with her bachelor's from the University of Central Florida in Electrical Engineer, December of 2023, currently working for Aldi's and looking to keep growing within that company after graduation.

Misael Salazar is planning to graduate with his bachelor's from the University of Central Florida in Computer Engineer, December of 2023, currently searching for his dream job, to become the best version of him at a place he could call home.

Tamara Nelson is planning to graduate with her bachelor's from the University of Central Florida in Photonics Engineer, December of 2023,

Kara Semmen is planning to graduate with her bachelor's from the University of Central Florida in Photonics Engineering, December of 2023, currently working for Lockheed Martin and looking to keep growing within that company after graduation.

Miguel Daboin is planning to graduate and receive his bachelor's degree in Electrical Engineering from the University of Central Florida in December of 2023. He is currently working for Siemens Gamesa Renewable Energy (SGRE) as a Hybrid Renewable Energy Systems Business Development Analyst and hopes to continue growing within that company after graduating.

ACKNOWLEDGEMENT

The authors wish to acknowledge the assistance and support of our sponsor Dr. Stephan Eikenberry.

We would also like to acknowledge and thank Dr. Arthur Weeks, who has provided so much assistance with the PCBs testing and soldering portion of the project.

We offer our thanks and gratitude to the professors who have so kindly agreed to be part of our Review Committee.

REFERENCES

[1] Wilken, T., et al. (2012). "A spectrograph for exoplanet observations calibrated at the centimetre-per-second level." Nature **485**(7400): 611-614.

[2] Reiners, A. (2010). "Detecting Planets Around Very Lowmass Stars With The Radial Velocity Method." The Astrophysical Journal(710): 432-443.

[3] Pradip Gatkine, S. V., Mario Dagenais (2019). "Astrophotonic Spectrographs." Applied Sciences.

[4] Tang, X. and X. Yan (2017). "Acoustic energy absorption properties of fibrous materials: A review." Composites Part A: Applied Science and Manufacturing **101**: 360-380.